COMPUTATION OF DIFFERENTIAL INVERSE MEAN FREE PATHS, INVERSE MEAN FREE PATHS AND STOPPING POWERS FOR ELECTRONS IN LIQUID WATER*

Franklin W. Hecker, Jr.

Centre College of Kentucky

Oak Ridge National Laboratory
Oak Ridge, Tennessee 37830

April 25, 1977

Prepared in partial fulfillment of the requirements of the ORNL-SCUU Science Semester under the direction of Dr. R. H. Ritchie, Research Adviser, in the Health and Safety Research Division.

*Research sponsored jointly by the Southern College University Union and the Energy Research and Development Administration under contract with the Union Carbide Corporation.

COMPUTATION OF DIFFERENTIAL INVERSE MEAN FREE PATHS, INVERSE MEAN FREE PATHS, AND STOPPING POWERS FOR ELECTRONS IN LIQUID WATER

ABSTRACT

A new numerical integration procedure has been developed to compute differential inverse mean free paths for electrons in water, and has been incorporated into a code which calculates inverse mean free paths and stopping powers. Relativistic and exchange corrections have been included.

I. INTRODUCTION

A Monte Carlo code simulating the transport of electrons in liquid water has been developed by Hamm and others[1] utilizing the differential inverse mean free paths (DIMFP's) and inverse mean free paths (IMFP's) for inelastic collisions. The procedure previously used to calculate DIMFP's for this code has been found to produce serious errors at large energy transfers (above 10 keV). I have developed a new procedure for calculating DIMFP's free from these errors, and have used this procedure to calculate IMFP's and stopping powers.

The total inelastic IMFP and DIMFP are given in the first Born approximation by[2]

$$\mu(E) = \int_0^E \frac{d\mu}{d\omega}(E,\omega) = \frac{1}{\pi E} \int_0^E \int_{\sqrt{2E}-\sqrt{2(E-\omega)}}^{\sqrt{2E}+\sqrt{2(E-\omega)}} \frac{dq}{q} \operatorname{Im}\left(\frac{-1}{\varepsilon(\omega,q)}\right) \qquad (1)$$

where E is the non-relativistic kinetic energy of the electron and $\varepsilon(\omega,q)$ is the dielectric response function for energy transfer ω and momentum transfer q. Exchange effects and relativistic corrections are not included in (1).

The dielectric response function used is given by[1]

$$\varepsilon_1(\omega,q) = 1 + E_p^2 \sum_n^{ex} f_n^{ex}(q) \frac{E_n^2 - \omega^2}{(E_n^2 - \omega^2)^2 + \gamma_n^2\omega^2} + E_p^2 \sum_n^{ion} f_n^{ion}(q) \frac{(E_n + q^2/2)^2 - \omega^2}{[(E_n + q^2/2)^2 - \omega^2]^2 + \gamma_n^2\omega^2} \quad (2)$$

and

$$\varepsilon_2(\omega,q) = E_p^2 \sum_n^{ex} f_n^{ex}(q) \frac{\gamma_n\omega}{(E_n^2 - \omega^2)^2 + \gamma_n^2\omega^2} + E_p^2 \sum_n^{ion} f_n^{ion}(q) \frac{\gamma_n\omega}{[(E_n + q^2/2)^2 - \omega^2]^2 + \gamma_n^2\omega^2} \quad (3)$$

where $E_p^2 = 4\pi N_M = 0.062257$ and N_M is the number density of water molecules in the medium.

II. NUMERICAL COMPUTATION OF DIMFP'S

The original procedure for calculating DIMFP's, using a numerical integration routine based on the trapezoid rule, was sufficiently accurate for low energy transfer ω, but was subject to large errors for high ω (above 10 keV). These errors were not of great importance in calculating $\mu(E)$ since for large ω $\frac{d\mu}{d\omega}$ behaves as $\frac{1}{\omega^2}$, and the contributions to $\mu(E)$ from this region will be relatively small. However, in calculating the stopping power

$$-\frac{dE}{dx} = \int_0^E \omega \frac{d\mu}{d\omega} d\omega \quad (4)$$

the effect of the errors is greatly increased by the presence of the multiplicative factor ω, resulting in computational errors of up to 10% and making difficult a meaningful comparison with experimental data and other

theoretical calculations. Inaccuracies in integration procedures also hampered proper evaluations of the chosen response function, such as verification of applicable sum rules and investigation of behavior at high energy transfer.

Obtaining accurate values for $\frac{d\mu}{d\omega}$ from numerical integration is difficult because the function $\frac{1}{q}\mathrm{Im}\left(\frac{-1}{\varepsilon(\omega,q)}\right)$ is very peaked for large ω in the region of the Bethe ridge. For example, for ω = 90 keV the region in which the function has more than 0.1% its maximum value has a width of 0.8, while a typical integration interval over q has width on the order of a hundred. This behavior produces two main types of error in approximating the integral of $\frac{1}{q}\mathrm{Im}\left(\frac{-1}{\varepsilon(\omega,q)}\right)$. First, if equal subdivisions are used in forming the approximating sum then only a few points in the vicinity of the peak will be accounted for. For example, if E = 100 keV and ω = 90 keV, and if the number of subdivisions is 500 (a typical value), then the width of the intervals will be 0.1 and only about ten points will be located in the peak region, far too few to give accurate results. Greatly increasing the number of subdivisions is impractical in terms of the time involved, since computing $\mathrm{Im}\left(\frac{-1}{\varepsilon(\omega,q)}\right)$ using (2) and (3) is a lengthy procedure.

Second, the function $\frac{1}{q}\mathrm{Im}\left(\frac{-1}{\varepsilon(\omega,q)}\right)$ is highly exponential in character, as can be seen in Fig. 1, and methods such as the trapezoid rule and Simpson's rule, which are based on approximating the function with polynomials, are inherently ill-suited to this problem.

Thus a method for calculating $\frac{d\mu}{d\omega}$ was sought that would give accurate results at high ω and use only a moderate number of integration points. After much experimenting a procedure was developed which satisfies the above requirements. This procedure has two main features, corresponding to the problems mentioned above. First, methods based on polynomial approximations were abandoned, and the integral of $\frac{1}{q}\mathrm{Im}\left(\frac{-1}{\varepsilon(\omega,q)}\right)$

over an interval (q_1, q_2) approximated by the area under an exponential function $f(q) = e^{aq+b}$, where $f(q_1) = \frac{1}{q_1} Im\left(\frac{-1}{\varepsilon(\omega,q_1)}\right)$ and $f(q_2) = \frac{1}{q_2} Im\left(\frac{-1}{\varepsilon(\omega,q_2)}\right)$. This area is $(q_2 - q_1)(f(q_2) - f(q_1))/(\log(f(q_2)) - \log(f(q_1)))$. An approximation of this kind, besides conforming more closely to the actual behavior of $\frac{1}{q} Im\left(\frac{-1}{\varepsilon(\omega,q)}\right)$, also has the advantage of using only one interval at a time, unlike Simpson's rule and other rules using higher degree polynomials. The additional computer time necessary to evaluate the logarithms is not important since it is small in comparison to the time required to evaluate $Im\left(\frac{-1}{\varepsilon(\omega,q)}\right)$ for each point.

The second feature involves abandoning the use of equal subdivisions and making the interval width used dependent on the slope of the function, so that more intervals will be used in the vicinity of the peak. After approximating the integral over the interval (q_1, q_2) as described above the next point used is given by $q_3 = q_2 + \delta$, where

$$\delta = \sqrt{2\alpha \left| \frac{q_2 - q_1}{f(q_2) - f(q_1)} \right|}$$

α being an adjustable error parameter specific for a given ω. Thus if the function is increasing (or decreasing) rapidly in a given region, so that the absolute value of the slope is large, then the interval width will be small. This procedure is based on an analysis of the error possible when using the trapezoid rule to integrate a monotonic function, but is actually used empirically, with the parameter α being chosen by trial and error. That is, $\frac{d\mu}{d\omega}$ is calculated several times for a specific ω, using a smaller value of α each time until sufficient accuracy is obtained. This is repeated for other representative values of ω, and an equation obtained through least squares analysis which, for a given ω, gives the appropriate parameter α. This process was carried out for ω

from 7.4 eV (taken as the ionization threshold) to 100 keV (using a primary energy E of 100 keV) and later extended to the region from 100 keV to 300 keV (using E = 300 keV). Parameters computed from this equation should be appropriate for any value of E less than 300 keV, since decreasing E for a given ω merely reduces the interval over q (and thus reduces the number of points used in the approximation). However, it was decided to introduce a factor reducing α for small E in order to keep the number of points used roughly equal to the number used at higher E and also to improve accuracy somewhat.

The main disadvantage of the procedure outlined above is obviously the need to determine the appropriate error parameters by trial and error (although once completed the process should not need to be repeated). There are also other smaller problems. For example, since the length of an interval is determined by the results from the previous interval, the first interval must be determined separately. Also, a lower limit on interval widths is necessary, to prevent using too many intervals, as is an upper limit, to prevent using too few intervals and skipping over the peak region. These modifications have been incorporated into the procedure.

The integration routine as presently formulated gives accurate results for $\frac{d\mu}{d\omega}$ (to within 0.5% or less) over a wide range of ω, and is fairly independent of the specific form of $\mathrm{Im}\left(\frac{-1}{\varepsilon(\omega,q)}\right)$. The average number of intervals used is between 100 and 500 depending on E.

As a final note, it was found that the previously used computation of $\mathrm{Im}\left(\frac{-1}{\varepsilon(\omega,q)}\right)$ was subject to some inaccuracies in the peak region (the denominators in (2) and (3) are then small and round-off error can occur). Thus all the variables involved in the computation of $\mathrm{Im}\left(\frac{-1}{\varepsilon(\omega,q)}\right)$ were con-

verted to double precision type. To further ensure accuracy all variables involved in the integration of $\frac{1}{q}Im\left(\frac{-1}{\varepsilon(\omega,q)}\right)$ were also changed to double precision.

III. NUMERICAL COMPUTATION OF IMFP'S AND STOPPING POWERS

In computing $\mu(E)$ and $\frac{dE}{dx}$ from (1) and (4) the functions $\frac{d\mu}{d\omega}$ and $\omega\frac{d\mu}{d\omega}$ are integrated using approximation with exponential functions of the form $g(\omega) = e^{a\omega+b}$ in a similar procedure to that described above. However it was not deemed necessary to use an interval determining method based on an error parameter. Instead the values of ω used in the approximating sum are entered as data, as was done previously, with the values so distributed so as to give an adequate number of points in the region where $\frac{d\mu}{d\omega}$ has its peak (from about 15 eV to 80 eV). I feel the convenience of this arrangement in printing out results outweighs any lack of flexibility present.

In an exception to the above method, the last value of ω is not taken to be E (for which $\frac{d\mu}{d\omega}$ vanishes) but rather 99.9% of E. The first value of ω used in (1) and (4) (and in all other integrations over ω where zero is the stated lower limit) is taken to be 7.4 eV.

IV. EVALUATION AND MODIFICATION OF THE CODE

To verify the suitability of the response function given by (2) and (3) a number of computation were made to ascertain if $Im\left(\frac{-1}{\varepsilon(\omega,q)}\right)$ satisfied applicable sum rules and showed the appropriate classical behavior in the region of high energy transfer.

The two sum rules used were

$$\int_0^\infty \omega Im\left(\frac{-1}{\varepsilon(\omega,q=0)}\right)d\omega = 2\pi^2 n \qquad (5)$$

and

$$\int_0^\infty \omega \log\omega \, \mathrm{Im}\left(\frac{-1}{\varepsilon(\omega,q=0)}\right) d\omega = 2\pi^2 n \log I \qquad (6)$$

where n = 0.04957 is the electron density in the medium and I is the mean excitation energy. Using an upper limit of 300 keV in (5) a value of 0.9800 was obtained for the integral, while $2\pi^2 n = 0.9785$. Using an upper limit of 300 keV in (6) the value I = 71.0 eV was obtained, compared to the value I = 65.1 eV used by Berger.[3]

For a classical electron-electron collision $\frac{d\mu}{d\omega} = \frac{\pi n}{\omega^2 E}$.[4] The DIMFP's computed by the code should approach this at high ω, for which the binding energy of the secondary electron can be neglected; this behavior is seen in Fig. 2. For example, for E = 100 keV and ω = 90 keV $\omega^2 \frac{d\mu}{d\omega} E = 0.1560$, compared to $\pi n = 0.1557$. For E = 60 keV and ω = 50 keV $\omega^2 \frac{d\mu}{d\omega} E = 0.1568$. The previously used routine for calculating $\frac{d\mu}{d\omega}$ was too inaccurate to show this (Fig. 3).

Thus the scheme for calculating DIMFP's shows the proper classical behavior at high energy transfers. However, it is in this region (10 keV and above) that relativistic and exchange effects become increasingly important. To include relativistic effects both the response function and the expression for $\frac{d\mu}{d\omega}$ were modified. In the response function free-electron like dispersion of ionization losses is still present, but the relativistic relation between kinetic energy and momentum is used. The relativistically corrected response function is given by

$$\varepsilon_1(\omega,q) = 1 + E_p^2 \sum_n^{ex} f_n^{ex}(q) \frac{E_n^2 - \omega^2}{(E_n^2-\omega^2)^2 + \gamma_n^2\omega^2} + E_p^2 \sum_n^{ion} f_n^{ion}(q) \frac{\left(E_n + c^2\sqrt{1+q^2/c^2} - c^2\right)^2 - \omega^2}{\left[\left(E_n + c^2\sqrt{1+q^2/c^2} - c^2\right)^2 - \omega^2\right]^2 + \gamma_n^2\omega^2} \qquad (7)$$

and

$$\varepsilon_2(\omega;q) = E_p^2 \sum_n^{ex} f_n^{ex}(q) \frac{\gamma_n \omega}{(E_n^2-\omega^2)^2+\gamma_n^2\omega^2} + E_p^2 \sum_n^{ion} f_n^{ion}(q) \frac{\gamma_n \omega}{[(E_n + c^2\sqrt{1+q^2/c^2} - c^2)^2 - \omega^2]^2 + \gamma_n^2\omega^2} \tag{8}$$

The relativistically corrected DIMFP is given by

$$\frac{d\mu(E,\omega)}{d\omega} = \frac{1}{\pi E}\frac{(1+E/c^2)^2}{(1+E/2c^2)} \int_{\sqrt{2E(1+E/2c^2)} - \sqrt{2E(1+E/2c^2) - 2\omega(1+E/c^2)+\omega^2/c^2}}^{\sqrt{2E(1+E/2c^2)} + \sqrt{2E(1+E/2c^2) - 2\omega(1+E/c^2)+\omega^2/c^2}} \frac{dq}{q} \mathrm{Im}\left(\frac{-1}{\varepsilon(\omega,q)}\right) \tag{9}$$

If $E \ll c^2$ ($E \ll$ 511 keV) then (7),(8) and (9) reduce to the expressions of (2), (3) and (1) respectively.

The stopping power with the effect of exchange included is calculated using

$$-\frac{dE}{dx} = \int_0^{E/2} d\omega \left\{ [\omega\mu'(E,\omega) + (E-\omega)\mu'(E,E-\omega)] - \left(\frac{E}{E+E_0}\right)^p \left[(E-2\omega)\mu'(E,E-\omega) + \omega\sqrt{\mu'(E,\omega)\mu'(E,E-\omega)}\frac{(1+2E/c^2)}{(1+E/c^2)^2} - \frac{\pi n\omega}{E(E+c^2)^2}\frac{(1+E/c^2)^2}{(1+E/2c^2)}\right]\right\} \tag{10}$$

where E_0 and p are constants and $\mu'(E,\omega)$ is calculated using (9). IMFP's are calculated using

$$\mu(E) = \int_0^{E/2} d\omega \left\{ [\mu'(E,\omega) + \mu'(E,E-\omega)] - \left(\frac{E}{E+E_0}\right)\left[\sqrt{\mu'(E,\omega)\mu'(E,E-\omega)}\frac{(1+2E/c^2)}{(1+E/c^2)^2} - \frac{\pi n}{E(E+c^2)^2}\frac{(1+E/c^2)^2}{(1+E/2c^2)}\right]\right\} \tag{11}$$

This scheme is obtained by analogy from the Möller formula[4]

$$\frac{d\mu}{d\omega} = \frac{\pi n}{E}\frac{(1+E/c^2)^2}{(1+E/2c^2)}\left[\frac{1}{\omega^2} + \frac{1}{(E-\omega)^2} - \frac{1}{\omega(E-\omega)}\frac{(1+2E/c^2)}{(1+E/c^2)^2} + \frac{1}{(E+c^2)^2}\right]$$

by replacing $\frac{\pi n}{E}\frac{(1+E/c^2)^2}{(1+E/2c^2)}\frac{1}{\omega^2}$ with $\mu'(E,\omega)$ and $\frac{\pi n}{E}\frac{(1+E/c^2)^2}{(1+E/2c^2)}\frac{1}{(E-\omega)^2}$ with $\mu'(E, E-\omega)$. The factor $\left(\frac{E}{E+E_o}\right)^p$ was introduced to take into account in some way the increasing importance of exchange effects for high energies and decreasing importance for low energies. If $E \ll E_0$ then the factor $\left(\frac{E}{E+E_o}\right)^p$ is negligible and (10) and (11) reduce in essence to (4) and (1).

Stopping powers calculated with and without consideration of exchange are shown in Table 1, along with the experimental data of Cole[5] (values for E = 50 keV and 100 keV were obtained from Berger[3]). The values for the complete exchange effect were obtained from (10) by replacing the factor $\left(\frac{E}{E+E_o}\right)^p$ with unity. For calculations involving a varying exchange effect (Fig. 4) E_0 = 3000 eV and p = 1; these values were chosen in order to obtain rough agreement with Cole's results. The agreement is not very good in the region below 1 keV; this reflects uncertainties both in experimental data and in the theoretical scheme.

V. CONCLUSION

A new procedure has been developed to accurately compute DIMFP's for electrons in liquid water, and has been incorporated into a code which calculates IMFP's and stopping powers. The code includes relativistic corrections to the dielectric response function $\varepsilon(\omega, q)$ and to the DIMFP, and is available in two versions, with or without exchange corrections. Thus far the code has been tested over a range of primary energies from 50 eV to 100 keV, and should be applicable to energies of

up to 1 MeV and above with minor modification. It may also be easily adapted to compute IMFP's and stopping powers for heavy ions in liquid water. The code and the integration procedure underlying it should thus improve the electron and heavy ion transport codes and permit a better evaluation of the theoretical dielectric response function for liquid water.

REFERENCES

1. R. N. Hamm, H. A. Wright, R. H. Ritchie, J. E. Turner, and T. P. Turner, "Monte Carlo Calculation of Transport of Electrons through Liquid Water", 1037-1053, Proceedings, Fifth Symposium on Microdosimetry.

2. Atomic units are used throughout unless otherwise specified. Energy is in units of e^2/a_0 = 27.212 eV, twice the ionization potential of hydrogen, and length is in units of a_0 = 0.5292 A, the Bohr radius.

3. M. J. Berger and S. M. Seltzer, "Tables of Energy Losses and Ranges of Electrons and Positrons", 205-268, Studies in Penetration of Charged Particles in Matter, NAS-NRC Publication 1133 (National Academy of Sciences-National Research Council, Washington, D.C., 1970).

4. R. D. Birkhoff, "The Passage of Fast Electrons through Matter", 53-138, Encyclopedia of Physics, Vol. XXXIV (Springer-Verlag, Berlin, 1958).

5. W. K. Sinclair, P. R. J. Burch, A. Cole, D. V. Cormack, W. Gross, and A. M. Kellerer, Linear Energy Transfer, ICRU Report 16 (International Commision on Radiation Units and Measurements, Washington, D.C., 1970).

Figure 1. $\frac{1}{q} \mathrm{Im}\left(\frac{-1}{\varepsilon(\omega,q)}\right)$ as a function of q for ω = 90 keV, in the peak region. Response function is non-relativistic.

Figure 2. $\omega^2 \frac{d\mu}{d\omega} E$ as a function of ω for E = 100 keV, calculated using the new integration procedure. Response function and expression for DIMFP are non-relativistic.

Figure 3. $\omega^2 \frac{d\mu}{d\omega} E$ as a function of ω for E = 100 keV, calculated using the previously used integration procedure. Response function and expression for DIMFP are non-relativistic.

Figure 4. Stopping power as a function of E, calculated using relativistically corrected DIMFP and response function and taking into account effects of exchange. Experimental points are from data of Cole.[5]

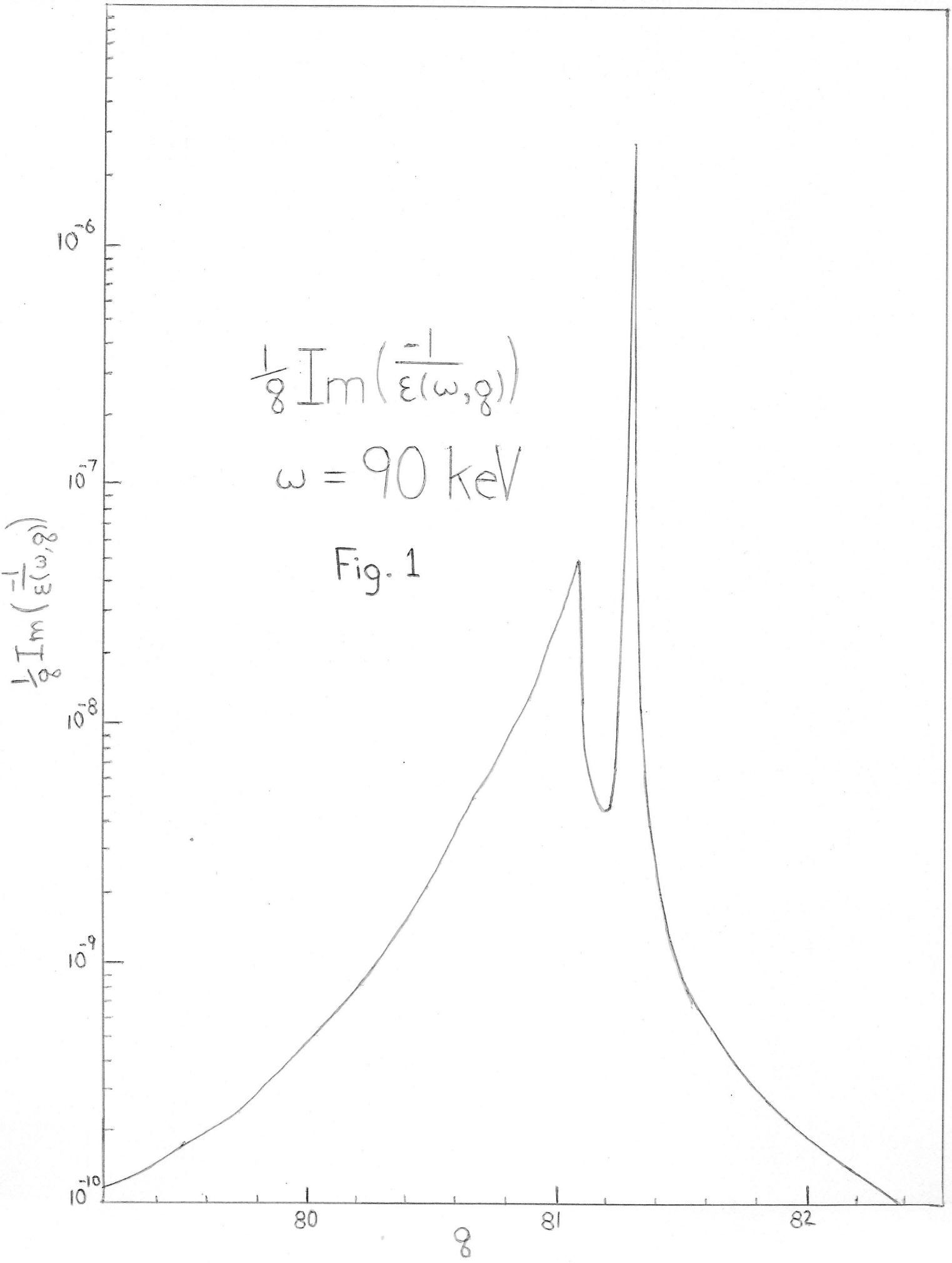
$\frac{1}{q}\,\mathrm{Im}\left(\frac{-1}{\varepsilon(\omega,q)}\right)$
$\omega = 90$ keV
10^{-6}
10^{-7}
10^{-8}
10^{-9}
10^{-10}
$\frac{1}{q}\,\mathrm{Im}\left(\frac{-1}{\varepsilon(\omega,q)}\right)$
80
81
82
q

Fig. 1

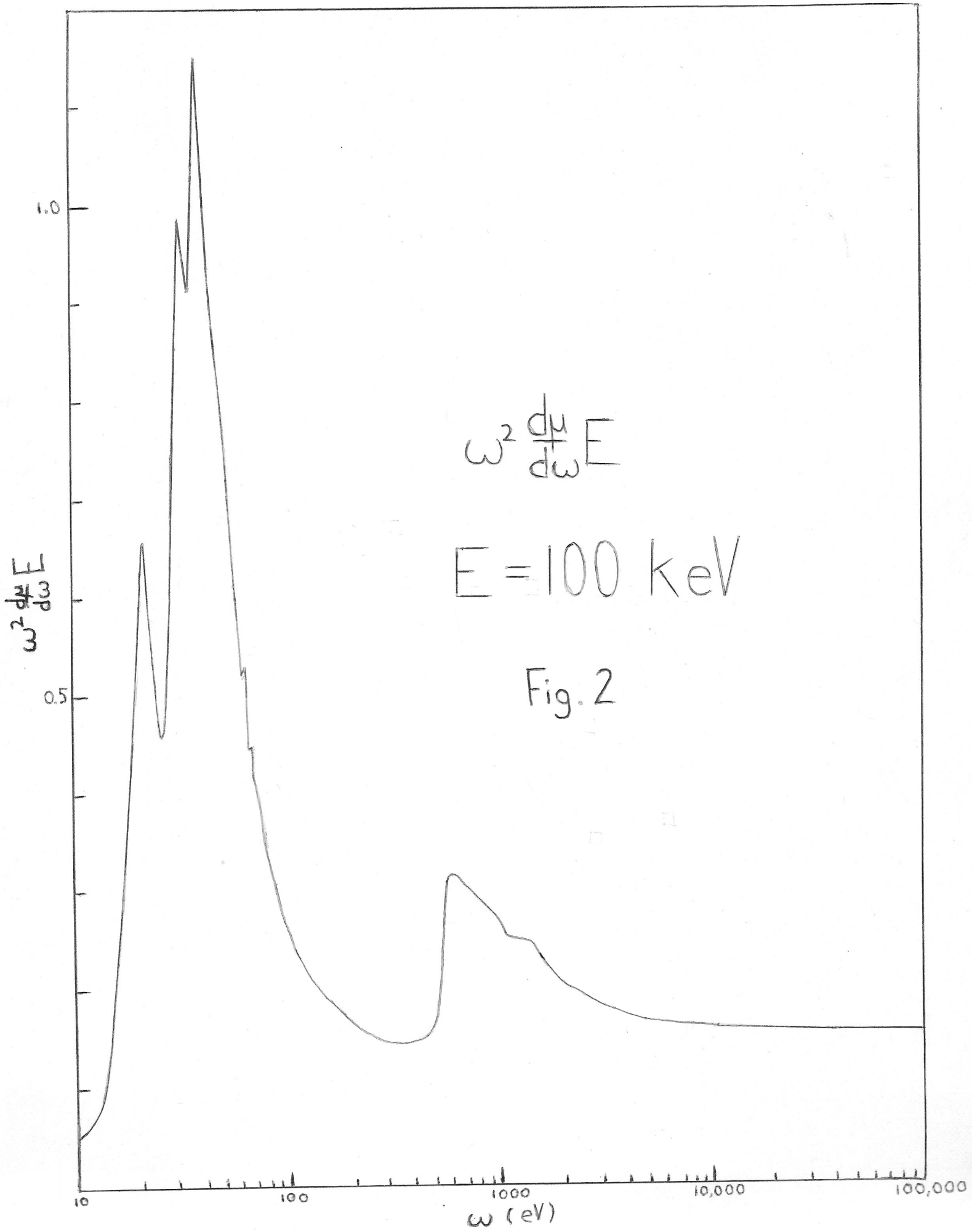

$\omega^2 \frac{d\mu}{d\omega} E$

$E = 100$ keV

Fig. 2

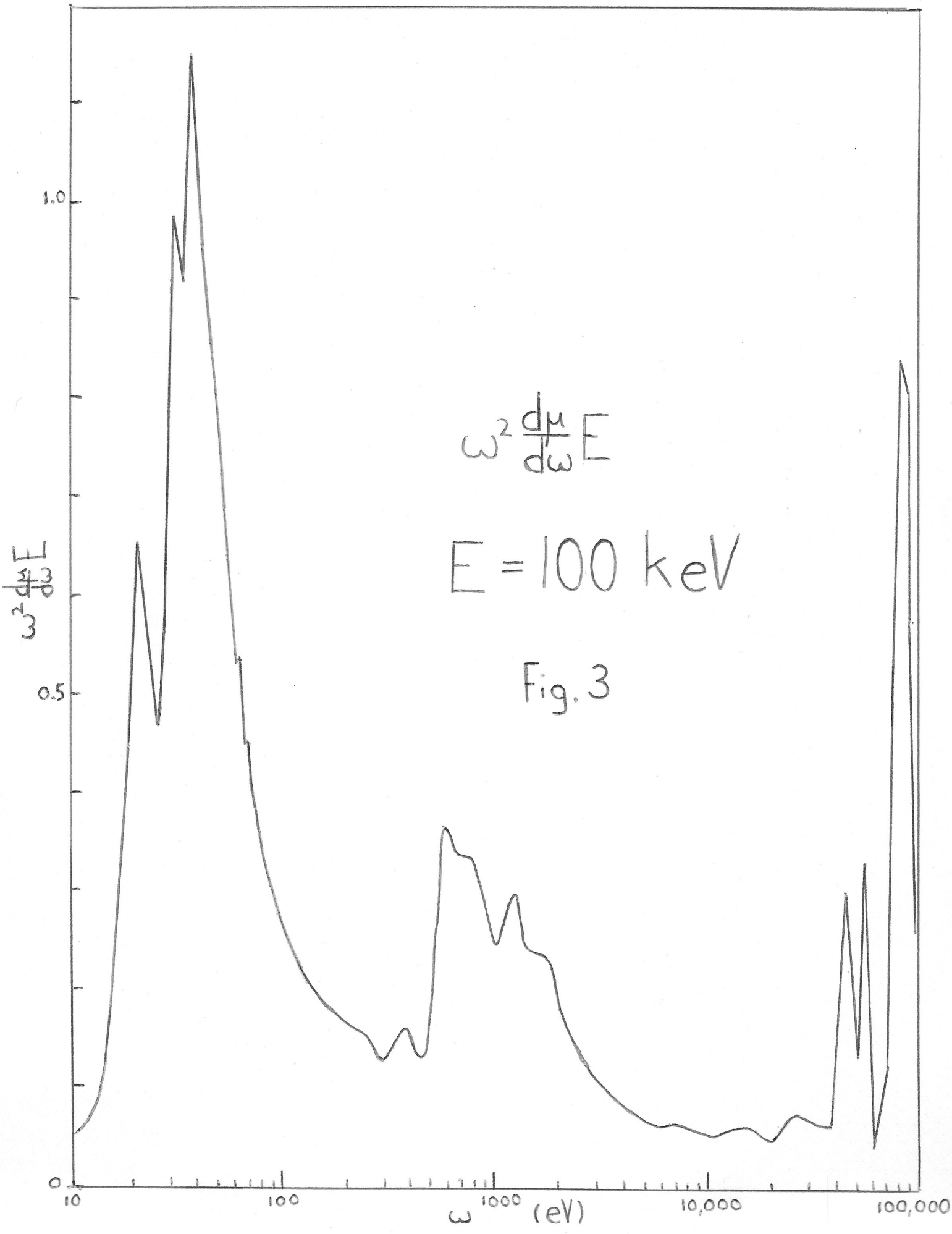
$\omega^2 \frac{d\mu}{d\omega} E$
E = 100 keV
Fig. 3
$\omega^2 \frac{d\mu}{d\omega} E$
1.0
0.5
0
10
100
1000
10,000
100,000
ω (eV)

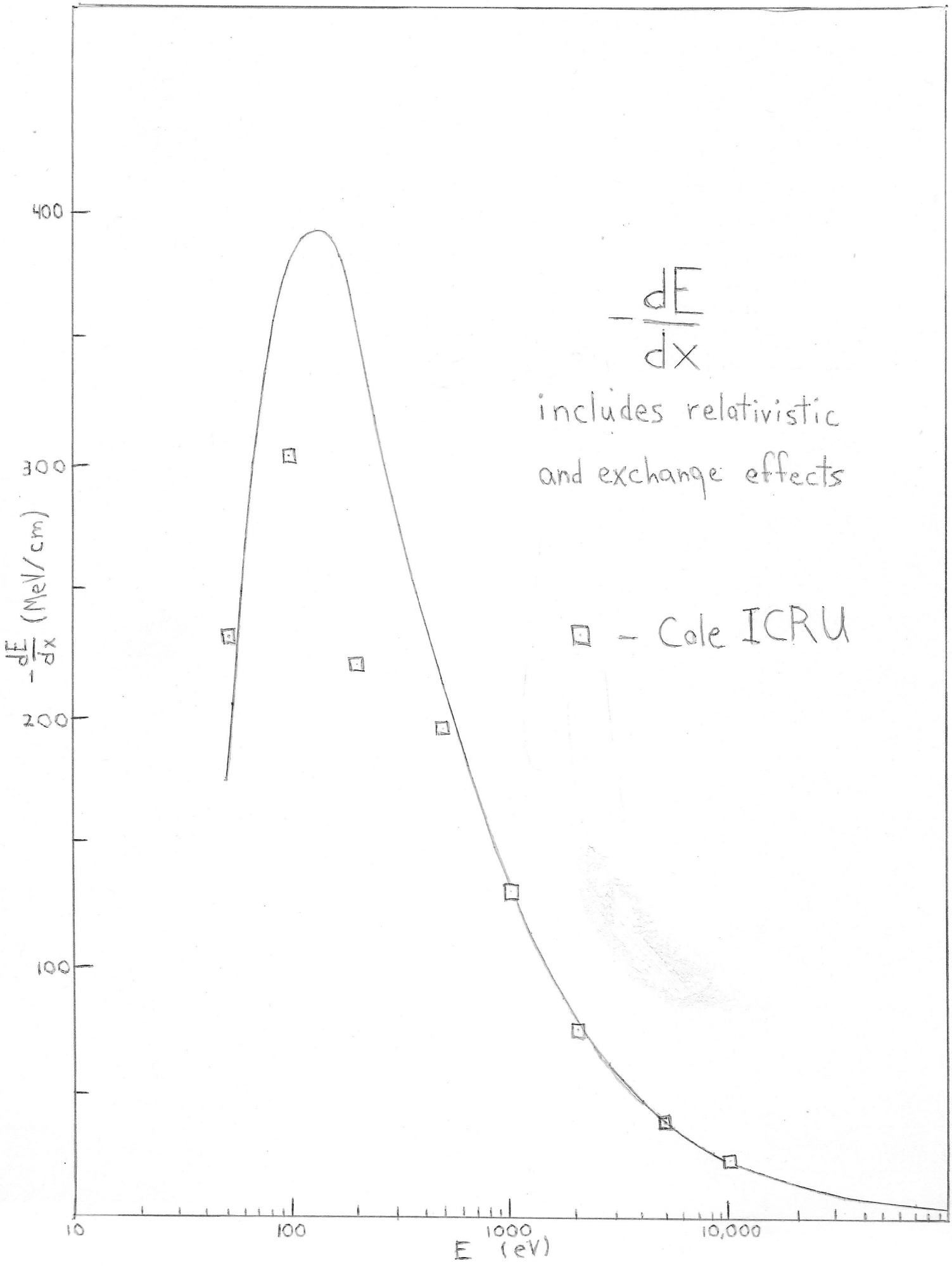
400
300
200
100
$-\frac{dE}{dx}$ (MeV/cm)
$-\frac{dE}{dx}$
includes relativistic
and exchange effects
□ - Cole ICRU
10
100
1000
10,000
E (eV)

E (eV)	$-\frac{dE}{dx}_{r,ne}$ (MeV/cm)	$-\frac{dE}{dx}_{r,ce}$ (MeV/cm)	$-\frac{dE}{dx}_{r,ve}$ (MeV/cm)	$-\frac{dE}{dx}_{Cole}$ (MeV/cm)
50	175.7	64.3	173.9	232.0
100	385.0	179.3	378.4	303.0
200	358.8	238.9	351.3	220.0
500	217.0	173.9	210.8	195.0
1000	134.6	113.9	129.4	130.0
5000	42.81	37.58	39.54	39.2
10,000	25.02	22.41	23.01	23.2
50,000	7.195	6.631	6.663	6.751[3]
100,000	4.450	4.135	4.144	4.202[3]

Table 1.

Stopping powers calculated using relativistically corrected DIMFP and with no exchange effect, complete exchange correction and varying exchange correction, and experimental stopping powers from data of Cole.[5] Values for E = 50 keV and 100 keV are from Berger.[3]